Solid State Communications 243 (2016) 28–35

Contents lists available at ScienceDirect

Solid State Communications

journal homepage: www.elsevier.com/locate/ssc

Communication

DFT and post-DFT studies of metallic MXY_3-type compounds for low temperature TE applications

M. Bilal [a,b], Saifullah [a,b], Iftikhar Ahmad [a,b,*], S. Jalali-Asadabadi [c], Rashid Ahmad [d], M. Shafiq [a,b]

[a] Center for Computational Materials Science, University of Malakand, Chakdara 18800, Pakistan
[b] Department of Physics, University of Malakand, Chakdara 18800, Pakistan
[c] Department of Physics, Faculty of Sciences, University of Isfahan (UI), Hezar Jerib Avenue, Isfahan 81746-73441, Iran
[d] Department of Chemistry, University of Malakand, Chakdara 18800, Pakistan

ARTICLE INFO

Article history:
Received 30 March 2016
Received in revised form
15 April 2016
Accepted 19 May 2016
Available online 8 June 2016

Keywords:
Low temperature thermoelectric materials
TE materials
Ab-initio calculations
Post-DFT studies

ABSTRACT

In this paper, thermoelectric properties of carbon and nitrogen based twenty metallic antiperovskites MXY_3 (M=Al, Ga, Ir, Mg, Pd, Pt, Rh; X=C, N; Y=Mn, Ni, Sc, Ti, Cr, Fe) using ab-initio density functional theory and post-DFT Boltzmann's techniques are investigated. The electronic properties of these compounds are also discussed. We find high values of Seebeck coefficient and small values of electronic thermal conductivity for $AlCTi_3$, $AlNSc_3$, $AlCNi_3$, $AlNTi_3$, $GaCCr_3$ and $MgCNi_3$ between −0.25 and 0.25 eV chemical potential. These results show high dimensionless figure of merit in metallic materials and therefore, we predict these materials can be potential candidates for low temperature thermoelectric applications.

1. Introduction

High temperature thermoelectric (TE) materials with large Seebeck coefficient are attractive for power generation. Large Seebeck coefficient is commonly observed in narrow band gap semiconductors with low carrier concentration [1] and therefore, narrow band gap semiconductors are extensively studied for this purpose. On the other hand low temperature TE materials, used in cooling, are not studied with the same seriousness as compared to the high TE materials, consequently the studies of the metallic TE materials are rare [2,3]. Lin et al. [4] reported the TE properties of metallic antiperovskites with a maximum experimental ZT value of 0.035 for SnC_xCo_3 around 250 K. Recently, we worked on the TE properties of metallic antiperovskites theoretically and observed that the Seebeck coefficient of $SnNCa_3$ enhances significantly with the effects of spin orbit coupling at room temperature [5]. The motivation of this work is to search low temperature TE materials in metallic antiperovskites, therefore we explore the TE properties of metallic compounds $AlCMn_3$, $AlCNi_3$, $AlCSc_3$, $AlCTi_3$, $AlCCr_3$, $AlNCr_3$, $AlNSc_3$, $AlNTi_3$, $GaCCr_3$, $GaCNi_3$, $GaCMn_3$, $GaNCr_3$, $IrNCr_3$, $MgCNi_3$, $MgNCr_3$, $PdNCr_3$, $PtNCr_3$, $PtNFe_3$, $RhNCr_3$ and $RhNFe_3$.

General formula of cubic antiperovskite materials is ABC_3, where A is divalent or trivalent element, B is carbon or nitrogen, and C is a transition metal [6,7]. Most of the antiperovskite materials are found in space group Pm3m (221), where A atom is located at the corners, B at the center and C at the faces of the unit cell [8]. Dense electronic states around the Fermi level in metallic antiperovskites make them good low temperature thermoelectric materials.

Thermoelectric properties are strongly dependent upon the thermal conductivity which consists of electronic and phonon parts. In semiconductors, phonons effects are prominent and electronic part of thermal conductivity is small. In metals, unlike semiconductors, contribution of phonons in thermal conductivity is a very small fraction of the total thermal conductivity and therefore can be safely neglected. Highest value of the lattice part of thermal conductivity in metals is at intermediate temperatures, i.e., between high and low asymptotic regimes, and even these highest values are lesser than 2%, [9,10] therefore for the metals under investigation, our studies are focused on their electronic part of thermal conductivities. Secondly, phonon drag increases effective mass of conducting electrons and can increase the Seebeck coefficient but it is only applicable for low temperatures ($T < 200$ K) [11].

* Corresponding author at: Center for Computational Materials Science, University of Malakand, Chakdara 18800, Pakistan.
E-mail address: ahma5532@gmail.com (I. Ahmad).

http://dx.doi.org/10.1016/j.ssc.2016.05.012
0038-1098/

2. Computational details

Density functional theory [12,13] based full potential linearized augmented plane waves (FP-LAPW) method as implemented in WIEN2k [14] is used to calculate electronic properties of the materials under consideration. The experimental values of lattice constants used as input parameters are taken from Refs. [15–22] to calculate theoretical lattice constants. The calculated relaxed lattice parameters are then used to calculate spin polarized electronic properties of these materials. For electronic properties, generalized gradient approximation (GGA) [23] is used to treat exchange-correlation effects. All materials show metallic nature, whereas the densities of states of these materials show that there are dense electronic states around their Fermi levels, which play critical role in transport properties. Separation energy of -6.0 Ry is used between the core and valence states for each compound. The wave functions inside the atomic spheres in the full potential scheme for these materials are expanded in terms of spherical harmonics up to $l_{max}=10$. The convergence parameter $R_{MT}K_{MAX}$, is set to 7. The RMT's used for these materials are presented in Table 1. In this method no shape approximation on either the potential or electronic charge density is made and space is partitioned into interstitial region (IR) and non overlapping muffin-tin (MT) spherical domains centered at the atomic sites. Muffin tin spheres are the ions within the unit cell whereas interstitial region contain the region among the ionic radii in the unit cell. The plane waves cutoff value for the charge density and potential is selected to be $G_{MAX}=12(Ry)^{1/2}$. For the electronic properties calculations 1000 special k-points are used in the irreducible wedge of the Brillouin zone (1WBZ).

Table 1
RMT's for each element of MXY_3 compounds.

Materials	Elements	RMT's	Materials	Elements	RMT's
$AlCMn_3$	Al	2.24	**$IrNCr_3$**	Ir	2.5
	C	1.5		N	1.59
	Mn	1.93		Cr	1.84
$AlCNi_3$	Al	2.2	**$MgCNi_3$**	Mg	2.33
	C	1.47		C	1.56
	Ni	1.89		Ni	2.01
$AlCSc_3$	Al	2.5	**$PdNCr_3$**	Pd	2.5
	C	1.8		N	1.6
	Sc	2.2		Cr	1.87
$AlCTi_3$	Al	2.48	**$PtNCr_3$**	Pt	2.5
	C	1.66		N	1.67
	Ti	2.03		Cr	1.94
$AlNSc_3$	Al	2.5	**$PtNFe_3$**	Pt	2.49
	N	1.82		N	1.55
	Sc	2.11		Fe	1.89
$AlNTi_3$	Al	2.4	**$RhNCr_3$**	Rh	2.49
	N	1.61		N	1.59
	Ti	2.1		Cr	1.85
$GaCMn_3$	Ga	2.4	**$RhNFe_3$**	Rh	2.42
	C	1.52		N	1.54
	Mn	1.96		Fe	1.88
$AlCCr_3$	Al	2.4	**$GaCNi_3$**	Ga	2.4
	C	1.52		C	1.52
	Cr	1.94		Ni	1.89
$AlNCr_3$	Al	2.4	**$GaNCr_3$**	Ga	2.4
	N	1.82		N	1.82
	Cr	1.85		Cr	1.94
$GaCCr_3$	Ga	2.4	**$MgNCr_3$**	Mg	2.33
	C	1.52		N	1.82
	Cr	1.94		Cr	1.94

Thermoelectric properties like Seebeck coefficients, electronic thermal conductivities and electrical conductivities are calculated using the calculated electronic properties by BoltzTraP code [24]. For the transport properties 100,000 k-points are used in IWBZ. The transport coefficients based on the rigid band approach to conductivity are explained by using the following Eq. (1):

$$\sigma_{\alpha\beta}(\varepsilon)=\frac{1}{N}\sum_{i,k}\sigma_{\alpha\beta}\left(i,\vec{\kappa}\right)\frac{\delta\left(\varepsilon-\varepsilon_{i,\vec{k}}\right)}{\delta(\varepsilon)} \tag{1}$$

$$\sigma_{\alpha\beta}\left(i,\vec{k}\right)=e^2\tau_{i,k}v_\alpha\left(i,\vec{k}\right)v_\beta\left(i,\vec{k}\right) \tag{2}$$

where N is the number of k-points and ε is the band energy. Eq. (2) explains k-dependent transport tensors, where τ is the relaxation time, and $v_\alpha\left(i,\vec{k}\right)$ is the component of group velocities. Transport coefficients, which are functions of temperature (T) and chemical potential (μ), i.e. electrical conductivity, Seebeck coefficient tensors and electronic thermal conductivity can be obtained by integrating the transport distribution [24,25]:

$$\sigma_{\alpha\beta}(T,\mu)=\frac{1}{\Omega}\int\sigma_{\alpha\beta}(\varepsilon)\left[-\frac{\partial f_0(T,\varepsilon,\mu)}{\partial\varepsilon}\right]d\varepsilon \tag{3}$$

$$S_{\alpha\beta}(T,\mu)=\frac{1}{eT\Omega\sigma_{\alpha\beta}(T,\mu)}\int\sigma_{\alpha\beta}(\varepsilon)(\varepsilon-\mu)\left[-\frac{\partial f_0(T,\varepsilon,\mu)}{\partial\varepsilon}\right]d\varepsilon \tag{4}$$

$$\kappa^0_{\alpha\beta}(T,\mu)=\frac{1}{e^2T\Omega}\int\sigma_{\alpha\beta}(\varepsilon)(\varepsilon-\mu)^2\left[-\frac{\partial f_0(T,\varepsilon,\mu)}{\partial\varepsilon}\right]d\varepsilon \tag{5}$$

$$\kappa_e=\kappa^0-S^2\sigma T \tag{6}$$

where α and β are the tensor indices, e is the electron charge, Ω is the volume of the unit cell, μ is the carrier concentration and f_0 is the Fermi-Dirac distribution function. The relaxation time, τ, is kept constant in this study. It is assumed to be a constant, based on the consideration that the electrons contributing to transport are in a narrow energy range due to the delta-function like Fermi broadening. The relaxation time is nearly the same for the electrons in such a narrow energy range. The validity of this method is tested earlier, and the method actually turns out to be a good approximation even for anisotropic systems [24–26]. Seebeck coefficient is calculated by the band structure calculations as it does not depend on the relaxation time (under the assumption that τ is constant) but electrical conductivity needs to be calculated with respect to the relaxation time. Although there is no limitation to increase the temperature theoretically using the BoltzTrap code but experimentally it is not acceptable to increase the temperature without taking the phases of the compounds under study into account. By this we mean that one has to be aware and careful about possible phase transitions by increasing the temperature. In other words, the temperature can be increased, if the band structures of the systems are not substantially changed. Thus, in our work the temperature is theoretically increased by the assumption that the bands of the systems are not significantly changed.

3. Results and discussion

3.1. Electronic properties

Total and partial densities of states of the selected materials are presented in Fig. 1 in spin up and spin down states. Figure presents density of states for $RhNFe_3$ and $AlCMn_3$. The values of density of states near Fermi level are small in spin down states as compared to spin up states. It is clear from the figure that the conduction band is mostly composed of p-states of nitrogen and carbon in $RhNFe_3$ and $AlCMn_3$, respectively. TE properties depend on the density of electronic states near Fermi level. We can see that top of valence band in $RhNFe_3$ is composed of Rh-d states. Similarly, in $AlCMn_3$ Mn-dz_2 and Mn-dxz+dyz states have peaks near Fermi level. Therefore, these states play important role in TE properties of these materials.

3.2. Thermoelectric properties

3.2.1. Seebeck coefficient

Seebeck coefficient is an important tool, which provides a sensitive test of the electronic structures of the materials in close proximity to the Fermi energy. Large values of Seebeck coefficient are desired for efficient TE devices. Fig. 2 presents Seebeck coefficients for $AlCMn_3$, $AlCTi_3$, $AlNSc_3$, $MgCNi_3$, $PtNCr_3$ and $AlCNi_3$ against chemical potential at 300, 600 and 900 K while the results for rest of the materials are presented in Supplementary data. The values of Seebeck coefficient lie between 25 and 100 μV/K. Seebeck coefficient of $AlNTi_3$ and $AlCTi_3$ approaches to 110 and 100 μV/K , respectively, at room temperature. Lin et. al [4] experimentally investigated thermoelectric properties of antiperovskites and presented $SnCCo_3$ with the Seebeck coefficient of 53 μV/K at 278 K. This is the largest Seebeck, not only among all antiperovskites materials but also in other metals like AuCo (−42 μV/K, 300 K), CuFe (−15 μV/K, 20 K), heavy Fermi metals $CeCu_2Si_2$ (34 μV/K, 200 K), $CeAl_3$ (42 μV/K, 50 K), $CePb_3$ (40 μV/K, 20 K), and $YbInCu_4$ (−30 μV/K, 50 K) [3]. Literature clearly shows our results are very significant in TE applications. For $AlCMn_3$ and $AlCTi_3$ we see better values of Seebeck coefficient in p-type as compared to n-type region while for other materials we see similar behavior for both p-type and n-type regions. The results provided in the paper and the Supplementary data show that some materials have good thermoelectric properties in p-type and others in n-type region. In practice, materials have both charge carriers and the Seebeck depends on dominant carriers in the material. In purely p-type materials, Seebeck is positive and in n-type Seebeck is negative. Therefore, by Seebeck coefficient of the materials, we can predict about the dominant carrier concentration in a material and doping can enhance desired type of carriers. Thus, we can say that materials with better response in p-type region have holes while materials with better response in n-type region have electrons as the mobile carriers [1]. As $AlNTi_3$ and $AlCTi_3$ show highest thermopower therefore, we can predict that these materials will show better TE response than other materials discussed in this paper.

3.2.2. Electronic thermal conductivity

Conducting electrons and lattice vibrations are the two sources of heat transfer across a material. In metals, thermal conduction through electrons is dominant while in semiconductors, lattice vibration is mostly responsible for the conduction of heat [27]. Materials with small thermal conductivity are required to make thermoelectric generators, as we need to maintain temperature gradient across the material. Fig. 3 presents electronic thermal conductivity for $AlCMn_3$, $AlCTi_3$, $AlNSc_3$, $MgCNi_3$, $PtNCr_3$ and $AlCNi_3$ against chemical potential at 300, 600 and 900 K. Thermal conductivity is minimum around zero chemical potential and increases as chemical potential is increased. The materials will give high figure of merit in the region between −0.25 and 0.25 eV chemical potential as in this region thermal conductivities are

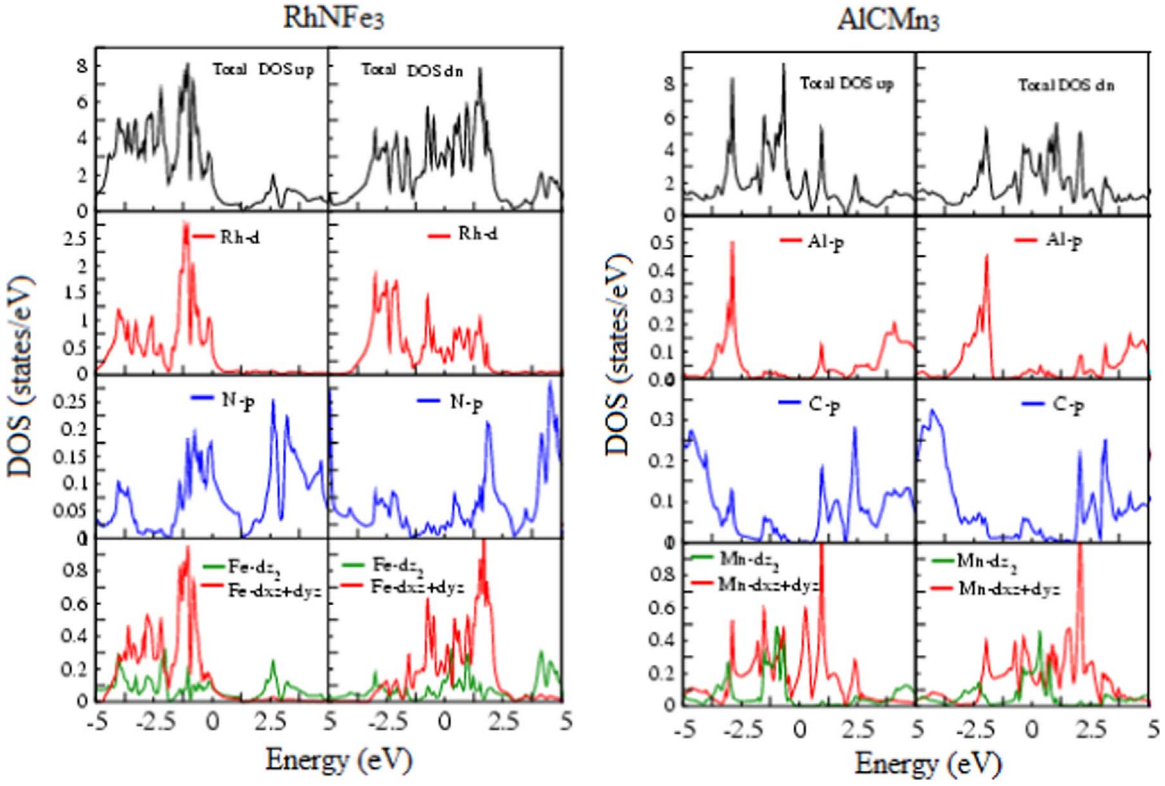

Fig. 1. Total and partial densities of states for $RhNFe_3$ and $AlCMn_3$ in spin up and spin down states.

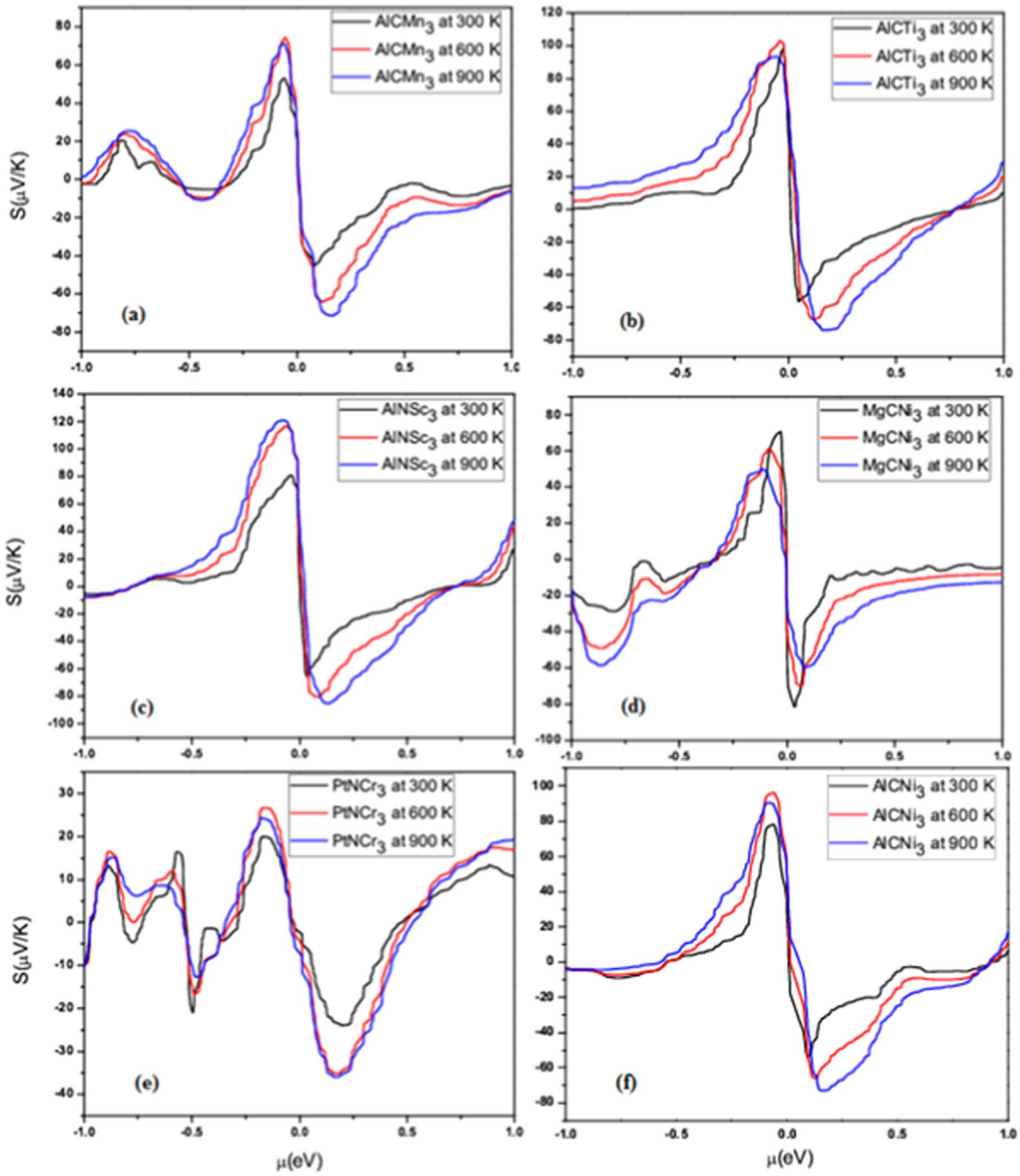

Fig. 2. Seebeck coefficients for (a) $AlCMn_3$, (b) $AlCTi_3$, (c) $AlNSc_3$, (d) $MgCNi_3$, (e) $PtNCr_3$ and (f) $AlCNi_3$ at 300, 600 and 900 K as a function of chemical potential.

minimum. Thermal conductivity increases when one moves away from $\mu=0$. Explanation for this may be given from the basic definition of chemical potential μ. When one atom is placed in an element and you want to place another, the first one will oppose the second. Similarly when a third atom is placed the first two will oppose. This opposition of the already placed atoms in an element or compound to the new incoming atoms is called chemical potential. When chemical potential increases then repulsion to the incoming atoms also increases, causing more lattice vibration. This increased lattice vibration results in high conductivity. Similarly, negative chemical potential means that a new entering atom is welcomed by the already present atoms in the element or compound and hence attraction occurs. Because of the attraction again lattice vibration increases as there is a force involved. This causes an increase in thermal conductivity. When chemical potential is negligibly small then repulsive or attractive force is also small resulting less vibrations and hence small conductivity [28]. The figure shows that $AlCNi_3$ and $AlNSc_3$ have the smallest electronic thermal conductivities. Further, we see an increase in thermal conductivity with temperature for all materials. Temperature increases electrons energy and as a result we get more transfer of heat.

3.2.3. *Electrical conductivity*

Flow of electrons from the high temperature region to the low temperature region in material results in electric current and this phenomenon is used to produce electrical energy in TE devices. Therefore, materials with high values of electrical conductivity are required for good TE generators. Fig. 4 presents electrical conductivity for $AlCMn_3$, $AlCTi_3$, $AlNSc_3$, $MgCNi_3$, $PtNCr_3$ and $AlCNi_3$,

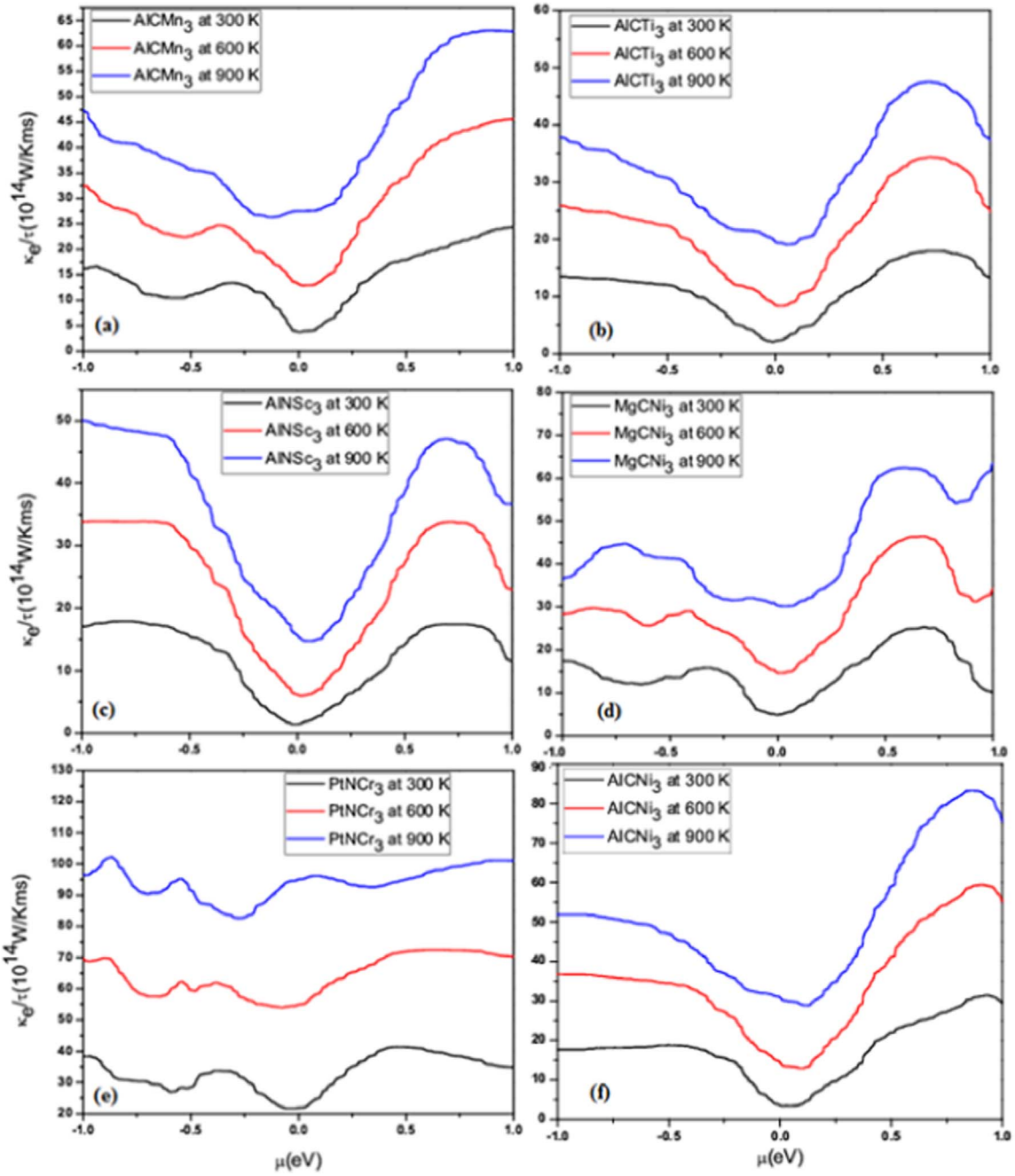

Fig. 3. Electronic thermal conductivities for (a) $AlCMn_3$, (b) $AlCTi_3$, (c) $AlNSc_3$, (d) $MgCNi_3$, (e) $PtNCr_3$ and (f) $AlCNi_3$ at 300, 600 and 900 K as a function of chemical potential.

against chemical potential at 300, 600 and 900 K. It is clear from the figure that electrical conductivity is maximum at higher values of chemical potential. $PtNCr_3$ gives the highest values of electrical conductivity near Fermi level. Further, we see that the values of electrical conductivity can be tuned by varying chemical potential.

3.2.4. Figure of merit

Figure of merit (ZT) is a parameter to determine the performance of a TE device, where it depends on high Seebeck coefficient, high electrical conductivity and low thermal conductivity. Materials with high value of ZT are desired for industrial applications. ZT greater than unity is considered very efficient in thermoelectric devices. Despite extensive research in thermoelectrics in recent years, scientists are still struggling to find such materials, which may replace conventional methods of energy production. Till now, $SnCCo_3$ (ZT=0.035 at 258 K) and $Sn_{0.95}Co_{0.05}CCo_3$ (ZT=0.04 at 258 K) have the largest figure of merits among all antiperovskites materials [4]. Table 2 presents the values of ZT at room temperature calculated in this work for $AlCMn_3$, $AlCNi_3$, $AlCSc_3$, $AlCTi_3$, $AlCCr_3$, $AlNCr_3$, $AlNSc_3$, $AlNTi_3$, $GaCCr_3$, $GaCNi_3$, $GaCMn_3$, $GaNCr_3$, $IrNCr_3$, $MgCNi_3$, $MgNCr_3$, $PdNCr_3$, $PtNCr_3$, $PtNFe_3$, $RhNCr_3$ and $RhNFe_3$. It is clear from the table that few materials show good thermoelectric response. The plots of figure of merit for $AlCMn_3$, $AlCTi_3$, $AlNSc_3$, $MgCNi_3$, $PtNCr_3$ and $AlCNi_3$, against chemical potential at 300, 600 and 900 K are shown in Fig. 5. It is clear from the figure that the peak values of ZT are found close to Fermi level. $AlNTi_3$ shows the highest value of figure of merit among these materials and it reaches to 0.32 at room temperature. This is due to the fact that this material has the highest values of the Seebeck coefficient and smallest electronic thermal conductivity. Large peaks of ZT between −0.25 and 0.25 eV chemical potential are due to the fact that Seebeck has large values while electronic

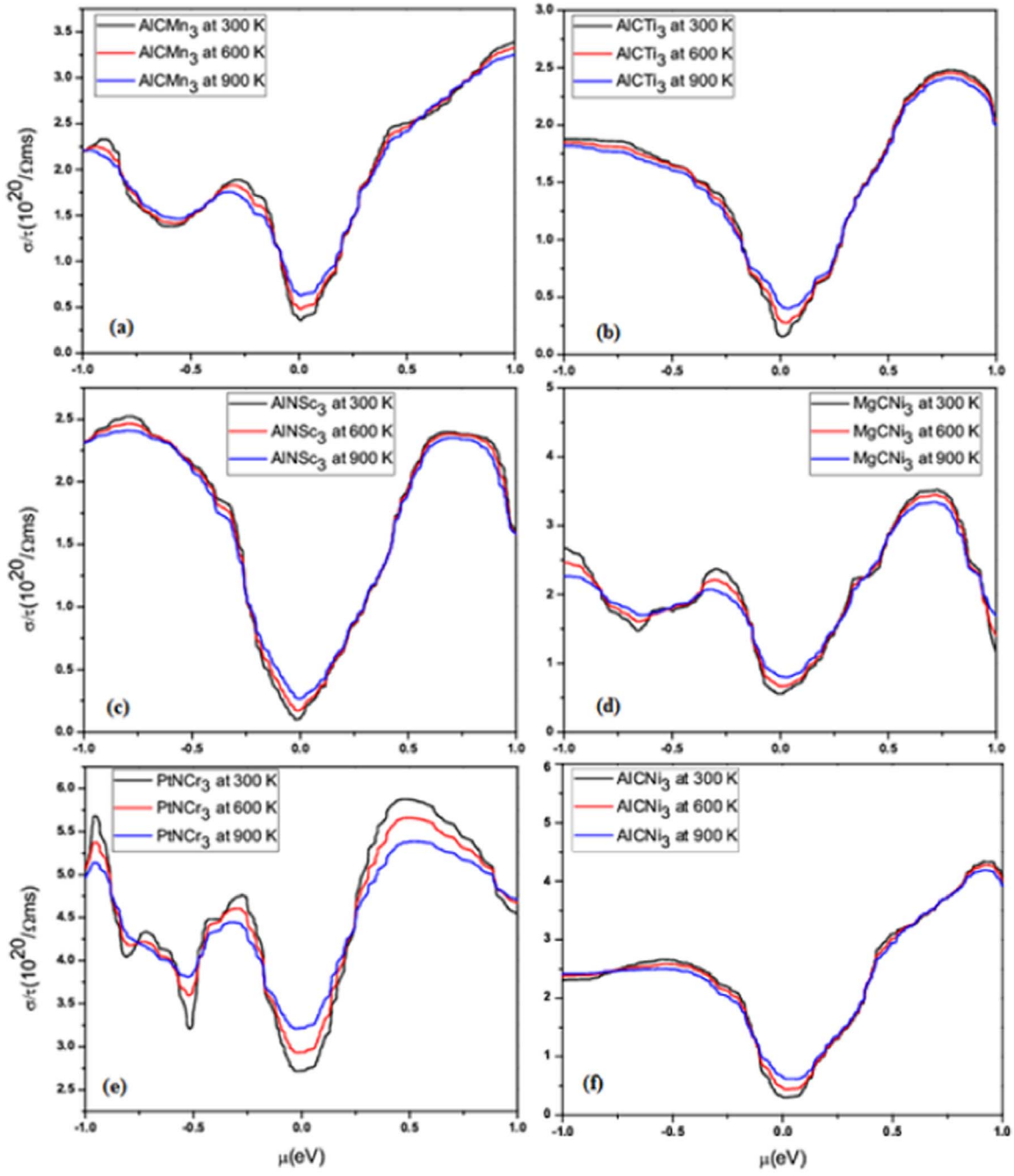

Fig. 4. Electrical conductivities for (a) $AlCMn_3$, (b) $AlCTi_3$, (c) $AlNSc_3$, (d) $MgCNi_3$, (e) $PtNCr_3$ and (f) $AlCNi_3$ at 300, 600 and 900 K as a function of chemical potential.

Table 2
Values of figure of merit (ZT) at room temperature for various metallic antiperovskites.

Materials	ZT	Materials	ZT
$AlCMn_3$	0.1	**$IrNCr_3$**	0.031
$AlCNi_3$	0.19	**$MgCNi_3$**	0.2
$AlCSc_3$	0.12	**$PdNCr_3$**	0.018
$AlCTi_3$	0.25	**$PtNCr_3$**	0.025
$AlNSc_3$	0.19	**$PtNFe_3$**	0.036
$AlNTi_3$	0.32	**$RhNCr_3$**	0.032
$GaCMn_3$	0.06	**$RhNFe_3$**	0.02
$AlCCr_3$	0.08	**$GaCNi_3$**	0.13
$AlNCr_3$	0.06	**$GaNCr_3$**	0.125
$GaCCr_3$	0.25	**$MgNCr_3$**	0.13

thermal conductivity has small values in this region. Small values of figure of merit, beyond this region, may be attributed to the large values of electrical conductivity. The comparison with the available data clearly shows that these materials may be useful in thermoelectric devices.

4. Conclusions

In this work we assessed the thermoelectric properties of twenty metallic antiperovskites, MXY_3 (M=Al, Ga, Ir, Mg, Pd, Pt; Rh, X=C or N; Y=Mn, Ni, Sc, Ti, Cr, Fe) and their electronic properties are also explored by using ab-initio calculations. It is concluded that $AlNTi_3$, $GaCCr_3$, $AlCNi_3$, $AlNSc_3$, $MgCNi_3$ and $AlCTi_3$ materials have relatively high values of Seebeck coefficient and

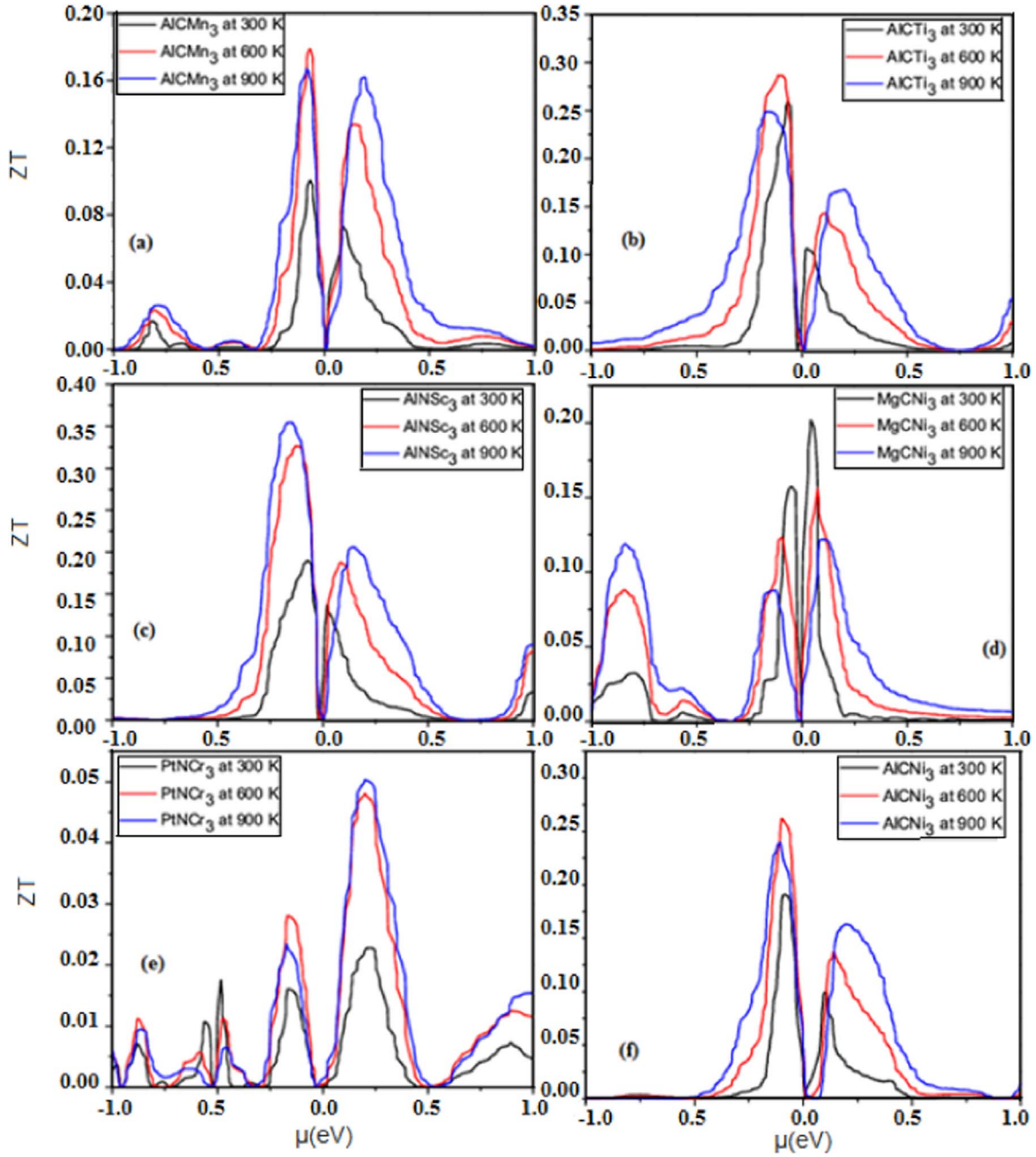

Fig. 5. Figure of merit for (a) $AlCMn_3$, (b) $AlCTi_3$, (c) $AlNSc_3$, (d) $MgCNi_3$, (e) $PtNCr_3$ and (f) $AlCNi_3$ at 300, 600 and 900 K as a function of chemical potential.

figure of merit with ZT values of 0.32, 0.25, 0.19, 0.19, 0.2 and 0.25 respectively, and hence are predicted to be low temperature thermoelectric materials.

Acknowledgment

We acknowledge the financial support from the Higher Education Commission of Pakistan (HEC), Project no. 20-3959/NRPU/R&D/HEC2014/119.

Appendix A. Supplementary material

Supplementary data associated with this article can be found in the online version at http://dx.doi.org/10.1016/j.ssc.2016.05.012.

References

[1] M.B. Ricoult, L.A. Moore, C.M. Smith, T.P. St Clair, Patent Application Publication, US 2014/0225022 A1, August 14, 2014.
[2] S.V. Ovsyannikov, V.V. Shchennikov, Chem. Mater. 22 (2010) 635.
[3] G.D. Mahan, Solid State Phys. 51 (1998) 81.
[4] S. Lin, P. Tong, B.S. Wang, J.C. Lin, Y.N. Huang, Y.P. Sun, Inorg. Chem. 53 (2014) 3709.
[5] M. Bilal, I. Ahmad, S.J. Asadabadi, R. Ahmad, M. Maqbool, Electron. Mater. Lett. 11 (2015) 466.
[6] J.B. Goodenough, J.M. Longo, K.H. Hellwege, O. Madelung (Eds.), Landolt–Bornstein, New Series, Group III, Springer-Verlag, Berlin, 1970, p. 126.
[7] K. Haddadi, A. Bouhemadou, L. Louail, F. Rahal, S. Maabed, Comput. Mater. Sci. 46 (2009) 881.
[8] V. Kanchana, S. Ram, Intermetallics 23 (2012) 39.
[9] C. Kittel, Introduction to Solid State Physics, eighth ed., John Wiley & Sons 2004, p. 156.
[10] T.M. Tritt, in: T.M. Tritt (Ed.), Thermal Conductivity: Theory, Properties, and Applications, kluwer academic/PLENUM publishers, 2004, p. 75.
[11] C. Kittel, Introduction to Solid State Physics, 7th ed., John Wiley and Sons Inc, 1996.

[12] O.K. Andersen, Phys. Rev. B 12 (1975) 3060.
[13] W. Kohn, L. Sham, Phys. Rev. 140 (1965) A1133.
[14] P. Blaha, K. Schwarz, G. Madsen, D. Kvasicka, J. Luitz, WIEN2k, An augmented plane wave plus local orbitals program for calculating crystal properties, Technical University of Vienna, Vienna, 2001.
[15] B.S. Wang, J.C. Lin, P. Tong, L. Zhang, W.J. Lu, X.B. Zhu, Z.R. Yang, W.H. Song, J. M. Dai, Y.P. Sun, J. Appl. Phys. 108 (2010) 093925.
[16] M. Sieberer, P. Mohn, J. Redinger, Phys. Rev. B 75 (2007) 024431.
[17] H. Holleck, Binäre und ternäre Carbide und Nitride der Übergangsmetalle und ihre Phasenbeziehungen, Institut für Material- und Festkörperforschung, Kernforschungszentrum Karlsruhe,1981.
[18] F. Grandjeant, A. Gerard, J. Phys. F: Metal Phys. 6 (1976) 451.
[19] Y. Medkour, A. Roumili, D. Maouche, A. Saoudi, Solid State Commun. 149 (2009) 1840.
[20] A. Houben, P. Müller, J. Appen, H. Lueken, R. Niewa, R. Dronskowski, Angew. Chem. 44 (2005) 7212.
[21] M.Y. Chern, D.A. Vennos, F.J. Disalvo, J. Solid State Chem. 96 (1992) 415.
[22] V. Kanchana, Euro. Phys. Lett. 87 (2009) 26006.
[23] J.P. Perdew, S. Burke, M. Ernzerhof, Phys. Rev. Lett. 77 (1996) 3865.
[24] G.K.H. Madsen, D.J. Singh, Comput. Phys. Commun. 175 (2006) 67.
[25] T.J. Scheidemantel, C. Ambrosch-Draxl, T. Thonhauser, J.V. Badding, J.O. Sofo, Phys. Rev. B 68 (2003) 125210.
[26] D. Wang, L. Tang, M.Q. Long, Z.G. Shuai, J. Chem. Phys. 131 (2009) 224704.
[27] O. Rabin, Y.M. Lin, M.S. Dresselhaus, Appl. Phys. Lett. 79 (2001) 81.
[28] M. Bilal, B. Khan, H.A. Rahnamaye-Aliabad, M. Maqbool, S. Jalali-Asadabadi, I. Ahmad, Comput. Phys. Commun. 185 (2014) 1394.